Colloid and Interface Science Communications 33 (2019) 100207

Contents lists available at ScienceDirect

Colloid and Interface Science Communications

journal homepage: www.elsevier.com/locate/colcom

Antibody conjugated green synthesized chitosan-gold nanoparticles for optical biosensing

Hasan Majdi[a], Roya Salehi[b,*], Mohammad Pourhassan-Moghaddam[c,d,e,**], Sahar Mahmoodi[c], Zahra Poursalehi[a], Steven Vasilescu[e]

[a] Department of Medical Nanotechnology, Faculty of Advanced Medical Science, Tabriz University of Medical Sciences, Tabriz, Iran
[b] Drug applied research center and Department of Medical Nanotechnology, Faculty of Advanced Medical Science, Tabriz University of Medical Sciences, Tabriz, Iran
[c] Department of Medical Biotechnology, Faculty of Advanced Medical Science, Tabriz University of Medical Sciences, Tabriz, Iran
[d] Institute for Biomedical Materials and Devices (IBMD), Faculty of Science, University of Technology Sydney, Sydney, NSW 2007, Australia
[e] School of Biomedical Engineering, University of Technology Sydney, Sydney 2007, Australia

ARTICLE INFO

Keywords:
LSPR
Dot blot
Nanobioprobe
Chitosan-gold nanoparticles
Antibody conjugation

ABSTRACT

In this study a novel antibody conjugated chitosan-gold nanoparticles (Ab-CS-GNPs) was engineered by the green synthesized method for detection of the target antigen (Ag) by three different types of optical biosensing system (colorimetric, localized surface plasmon resonance (LSPR) and paper-based dot-blot). Colloidal GNPs was synthesized by chitosan as reducer and stabilizer agent. For paper-based dot-blot detection, antibodies were conjugated to CS-GNPs surface and applied as nanobioprobe to the detection of spotted Ag on nitrocellulose (NC) membrane by the naked eye. Dot-blot assay results showed that the limit of detection (LOD) of the nanobioprobe is 1 μg/ml without any signal enhancement. In colorimetric and glasslide-based LSPR detections no significant response to antigen binding was observed due to the high thickness of chitosan layer on GNPs surface. Therefore, this engineered system could be used as nanobioprobe for optical detection of Ag in sandwich-like immunoassay systems that apply GNPs as a label of Ab.

1. Introduction

Antibody-conjugated gold nanoparticles are the most commonly used bio-modified nanomaterials in biomedicine, including therapeutics [1,2], diagnostics [3,4], and theranostics [5,6]. GNPs have unique physical, mechanical, electrical and optical properties that can be adjusted via changes in shape, size and dielectric constant; these features make them suitable for use in sensing and imaging applications [7–9]. Nevertheless, on their own, they cannot specifically detect targets and thus, there is a need for the application of moieties that confer selectivity to GNPs.

Therefore, more research is needed to design new methods for antibody immobilization onto GNP surfaces for implementation in sensitive and selective biosensing applications [10,11]. Biosensors, depending on the method of signal transduction, can be classified into various groups including thermometric, magnetic, electrochemical, piezoelectric and optical [12]. Optical biosensors are reported as the most commonly used biosensors. Many materials have been used to generate signals in optical sensors but Gold nanomaterials, due to their unique optical properties, are widely applied for use in optical biosensing [13,14]. Gold nanoparticles can be used in different configurations of optical detection such as paper-based [15,16], colorimetric [17,18], surface plasma resonance (SPR) [19], localized surface Plasmon resonance(LSPR) [20], dry-reagent strip [21], surface-enhanced Raman scattering (SERS) [22], chemiluminescence [23] and fluorescent [24].

Various common methods have been used to immobilize antibodies on the surface of gold nanoparticles, such as EDC/NHS coupling chemistry [25], electrostatic interaction [26,27], thiol reduction [7–10] and UV-NBS method and glutaraldehyde spacer method [28,29]. Among the many processes for antibody immobilization on GNP surfaces, chemical methods are commonly used for nanoparticle synthesis. The surface chemical moieties present on prepared GNPs, such as citrate and CTAB are directly replaced by functional antibodies (commonly in the thiol reduction and UV-NBS methods). In indirect replacement a compound contains functional groups attached to GNPs

* Corresponding author.
** Correspondence to: M P. Moghaddam, Department of Medical Biotechnology, Faculty of Advanced Medical Science, Tabriz University of Medical Sciences, Tabriz, Iran.
E-mail addresses: salehiro@tbzmed.ac.ir (R. Salehi), pourhassanm@tbzmed.ac.ir (M. Pourhassan-Moghaddam).

https://doi.org/10.1016/j.colcom.2019.100207
Received 11 May 2019; Received in revised form 16 August 2019; Accepted 9 September 2019
Available online 14 September 2019

surface and in next step can be conjugated to the antibody such as glutaraldehyde spacer and EDC/NHS methods [30]. Therefore, the conjugation of antibody to chemical-based nanoparticles requires several steps and also, the ligand exchange process is sometimes difficult due to weak stability of the nanoparticles in suspension during and after the coating process. A convenient way to the conjugate antibody to the GNP surface is to use functional polymers that, in addition to maintenance of the immobilized antibody on the surface, stabilize the GNPs colloidal suspension [2].

Chitosan is a linear polymer of [α (1 → 4)-linked 2-amino-2-deoxy-β-D-glucopyranose] derived by the *N*-acetylation of chitin. It is well known as a biocompatible and biodegradable natural polymer [31]. Chitosan molecules contain high numbers of reactive hydroxyl and amine groups that can be used for immobilization of biomolecules [32]. Hence it has been used as a gold nanoparticles coating, applied during synthesis [33,34] or after synthesis [35], for various biomedical applications such as photothermal therapy [35], drug delivery [36], gene delivery [37], and sensing [38].

Several studies have been reported the application of chitosan-gold nanomaterials for biomedical diagnosis. In some studies, the unmodified CS-GNPs were used for biodetection. For example, the catalytic activity of CS-GNPs in combination with the reaction of glucose oxidase was applied to detect glucose [39]. In another study, heparin detection was accomplished with the aid of CS-GNPs by observing the change in resonance light scattering (RLS) [35]. Another way to apply CS-GNPs for biomedical diagnostics is through the physical adsorption of biomacromolecules onto their surface. For example, *Mycobacterium tuberculosis* nucleic acid was colorimetrically detected through its physical adsorption on CS-GNPs [38]. In another study, antibodies against β-adrenergic agonist ractopamine (anti-RAC) were non-covalently immobilized on the surface of CS-GNPs for electrochemical immunoassay of RAC [40]. Also, some studies report the covalent immobilization of antibodies onto a CS film-GNP composite; the film was used to fabricate an Au microelectrode amperometric response immunesensor for detection of aflatoxin B1 (AFB1) [41]. In a similar study, an Ab-CS film-GNP conjugate was used for *Salmonella* detection through a glassy carbon electrode-based electrochemical immunesensor [42]. However, up to now, there is no report on direct covalent antibody immobilization on colloidal CS-GNPs surface and green synthesized GNPs.

The aim of this study is to provide a safe, rapid, low-cost, and equipment-free procedure for the stabilization and functionalization of green synthesized GNPs by antibody and to study its capability in optical biosensors. For this purpose, colloid gold nanoparticles were green synthesized using chitosan as a reducer and stabilizing agent. In the next step, we developed the antibody conjugated colloidal CS-GNPs as well as antibody conjugated glass slide-immobilized CS-GNPs. Furthermore, the usefulness of CS-GNPs for fabricating immunoassay-based optical biosensors was evaluated in three different biosensing systems including colorimetric, glasslide based LSPR and paper-based dot-blot assays.

2. Experimental section

2.1. Materials

Low molecular weight chitosan (50,000–190,000 Da), gold(III) chloridetrihydrate, phosphate buffered saline (PBS), (3-aminopropyl) triethoxysilane (APTES) (99%), EDC (1-Ethyl-3-(3 dimethylaminopropyl)-carbodiimide), NHS (N-hydroxysuccinimide), 3,3′,5,5’ Tetramethylbenzidine (TMB), Bovine serum albumin (BSA) and Horse Radish Peroxidase (HRP) were purchased from Sigma-Aldrich, Germany. Mouse IgG (used as antigen), HRP-tagged mouse IgG, HRP-tagged goat IgG and anti-mouse IgG antibody (Ab) produced in goat were purchased from Razi Institute, Iran. Tween-20, acetic acid, glutaraldehyde (GA), and nitrocellulose membrane were bought from Merck, Germany. Ultrapure deionized water (DI) (18.2 MΩ) (Millipore Synergy water purification system) was used for washing and preparation of solutions. All other chemicals were of analytical grade and used as received.

2.1.1. Synthesis of CS-GNPs in one step

All glassware was cleaned with deionized water and sonicated for 30 min in an ultrasonic bath (Wise clean, Digas.gr, Greece) before use. Chitosan was used as a reducing and stabilizing agent during the functionalization of gold nanoparticles by modification of a method provided by Huang, H. and X. Yang [34]. Typically, 500 mg of Chitosan was dissolved in 50 ml 1% (*v*/v) acetic acid and the reaction vessel was stirred by thermostatic magnetic stirring at 65 °C. Then, 50 mL of $HAuCl_4$ (1 mmol/L) solution was added to the reaction. After the suspension color turned purple gradually, the reaction temperature was kept at 65 °C for 2 h and then reduced to 25 °C while left stirring overnight. The synthesized CS-GNPs were centrifuged and diluted with deionized water and analyzed using UV–Vis spectroscopy (Cecil UV, UK). The molar concentration of synthesized GNPs was determined from the average GNP core diameter obtained from TEM and the calculated concentration of Au (0) atoms in the CS-GNPs solution [43,44].

2.1.2. Bio-conjugation of antibody on CS-GNPs surface

GA and EDC/NHS were used to conjugate Ab with the surface of CS-GNPs. Amine groups on the CS-GNPs and antibody readily combines with the functional aldehyde groups of GA. Furthermore, EDC/NHS was used to coupling of amine groups on the surface of CS-GNPs with carboxyl groups present in the Ab. Firstly, the solution of CS-GNPs was diluted with distilled water to the optical density (OD) = 0.4 (0.73 nM), and the pH of the solution adjusted to 5.5. GA was added to the solution at a final concentration of 2% (GA-CS-GNPs), and sonicated for 5 min in an ultrasonic bath, then, incubated for 2 h at 40 °C and again sonicated for another 5 min. In order to remove the residual GA, the mixture was washed several times with water by centrifugation. 0.3 mL of anti-IgG in various concentrations (0.01, 0.1, and 1 mg/ml) was added to the 0.7 mL GA-CS-GNPs solution and incubated at 4 °C for overnight. In the next step, in order to block the non-specific binding sites on the surface of the nanoparticles; BSA (5%) in PBS (0.01 M, pH 8.5) was incubated with the as-prepared conjugated at 20 °C for 45 min. Finally, the resultant conjugate was washed with PBS 0.01 M at pH 5, 7.4 and 9 (to remove physical adsorptions) then re-suspended in PBS and stored at 4 °C for future uses.

For the conjugation of Ab to CS-GNPs via EDC/NHS we adopted the method described by Narayan et al. [45]. Briefly, 1 mL of anti-IgG (Ab) with a concentration of 1 mg/ml was prepared and 1.5 mg of EDC and 1.1 mg NHS was added, mixed well and then, various concentrations (0.01, 0.1 and 1 mg/mL) of this solution was prepared. 0.3 mL of each concentration was added to the 0.7 mL CS-GNP solution and incubated at 4 °c for overnight. Then BSA (5%) was added for 45 min and finally, the solution was centrifuged to remove the excess BSA.

2.1.3. Measurement of refractive index sensitivity

Various ratios of water-glycerol mixture (*v*/v %) were used to change the refractive index of the surroundings of CS-GNPs and Ab-CS-GNPs. The volume of glycerol in the liquid mixture was varied from 0% to 75% in 15% increments. As-prepared CS-GNPs and Ab-CS-GNPs were first centrifuged at 6000 rpm for 8 min and then re-dispersed into the water-glycerol mixture. Then, UV–Vis spectra of the resulting dispersion solutions of nanoparticles were measured and the SPR shift as a function of the refractive index was plotted.

2.1.4. Colorimetric detection

In a typical experiment, 0.2 mL of PBS (pH = 7.4) and 0.4 mL Ab-CS-GNPs were mixed and incubated for 20 min at room temperature then UV–Vis spectra of the mixture was recorded as a control. In the test samples, 0.2 mL of mouse IgG solution at different concentrations (1 ng-

1 mg/mL) was added into the 0.4 mL Ab-CS-GNPs mixture and the solution was incubated for 20 min. Finally, the UV–Vis absorption spectra were recorded over the wavelength in the range of 400–800 nm.

2.1.5. Fabrication of glasslide

The microscope glasslides were cut to a size of 9 mm × 30 mm. For functionalization of glasslides we modified the method described by Chen et al. [46]. The slides were flushed several times with deionized water and then dried for 2 h at 120 °C under nitrogen flow. The washed glasslides were immersed in piranha solution (7 parts H_2SO_4 to 3 parts 30% H_2O_2) at 80 °C for half an hour. Then rinsed four times with DI water with simultaneous sonication and immediately dried at 120 °C for 2 h under nitrogen flow. The dried slides were dipped in an APTES solution (1% APTES in toluene) for 30 min, at 25 °C. Finally, the slides were sonicated for 5 min to take off the unbound APTES and subsequently washed several times with toluene, methanol, and deionized water and finally dried at 120 °C, under nitrogen flow. Silanized glass slides were stored in a vacuum for future uses.

2.1.6. Immobilization of CS-GNPs nanoparticle on glasslide surfaces and antibody conjugation

Firstly, the synthesized CS-GNPs were centrifuged and the remaining sediment diluted until the OD in maximum absorbance became 6. Then, silanized glass slides were immersed in a 5% GA (*W*/W) water solution for 30 min at 40 °C, to generate terminal aldehyde groups. The slides were then rinsed with water and dipped into the CS-GNP solution for 24 h to directly immobilize CS-GNPs on the glass surface via covalent bonding. In the next step, the CS-GNPs immobilized glasslides was washed several times with acetic acid (1 wt%) to remove non-absorbed nanoparticles. In order to conjugate the antibody to the CS-GNP surface, the chip was placed in a 5% GA solution in DI water at 40 °C for 3 h then washed several times with PBS. The chip was immersed in an anti-IgG solution (0.1 mg/ml in PBS) for 6 h at 4 °c. The fabricated chips were washed several times with PBS at PH 5, 7.4 and 9 to remove the non-conjugated antibody.

2.1.7. LSPR detection

Chips were immersed in a PBS solution for 30 min, and UV–Vis absorption spectra were recorded as a control. An Ag stock solution was diluted with PBS to obtain various concentrations. Next, 1 mL of the antigen solution in various concentrations was added to the chips and incubated for 30 min. Following a thorough wash with PBS the UV–Vis absorption spectra was recorded within a 400–800 nm wavelength range.

2.1.8. HRP-based assays

HRP enzyme was used as a protein to confirm the functionality of surface amine groups, their capability to bind protein in each step and estimate the number of functional antibodies per colloidal GNP. HRP-based assays were performed for three intentions.

2.1.9. Functionality of surface amine groups of colloidal CS-GNPs, silanized glasslide and CS-GNPs-glasslide

To this, colloidal CS-GNPs, silanized glasslide and CS-GNPs-glasslide were activated with the glutaraldehyde solution (4% *v*/v) for 45 min. After washing several times with DI water, they were treated with a solution of HRP and BSA as a control, with a final concentration of 0.1 mg/mL for 6 h at 4° for each sample. Finally, to remove unbound HRP and BSA, they were washed with a PBS (PH 7.4) solution three times and added TMB substrate to confirm presence of HRP.

2.1.10. Confirm the functionality of Ab on colloidal Ab-CS-GNPs and Ab-CS-GNPs-glasslide

The HRP-tagged mouse IgG and HRP-tagged goat IgG were added to samples as the target Ag and control, respectively. After washed well to remove unbound Ag, TMB substrate was added to all of the samples to confirm the conjugation and function of Ab.

2.1.11. Estimate the number of functional antibody per colloidal GNP

We used a method described by van der Heide S [9]. For this purpose, briefly, five standard solutions (in 400 µL volume) of HRP-tagged Ag, ranging in concentrations from 0 to 400 nM in 0.01 M PBS (pH 7.4) were prepared. Then, 200 µL of TMB substrate was added to each standard solution and incubated for 20 min in the dark place at room temperature. Subsequently, the stop solution (sulphuric acid 0.5 M in DI water) was added. The absorbance intensity of all samples was measured at 450 nm to draw the calibration curve. In the next step, a 10 µM of the HRP-tagged Ag was prepared in 0.01 M PBS (pH 7.4), after a while, 50 µL of this solution was added to 350 µL of Ab-CS-GNPs and incubated at room temperature for 30 min and then unbound HRP-tagged Ag were removed by repeated centrifugation and re-dissolving the pellet in 400 µL PBS (pH 7.4). The concentration of GNPs in this solution was determined by beer-lambert law. Eventually, 200 µL TMB substrate solutions were added and after 20 min incubation, it was centrifuged to remove the GNPs. The absorbance intensity of solution was recorded at 450 nm and the concentration of HRP-tagged Ag was determined using a standard calibration curve.

2.1.12. Paper-based dot-blot assay

In a typical experiment, 1 µl of each mouse IgG (Ag) solution (0.1, 1, 10, and 100 µg/mL) was spotted onto a nitrocellulose membrane and dried for 30 min at room temperature. Then, membranes were blocked with 3% BSA solution and air-dried for 30 min then washing with PBS. Finally, each sample was dipped into anti-mouse IgG (Ab)-CS-GNPs with OD of 1 at maximum absorbance (1.8 nM) and volume of 2 mL and after incubated for 20 min, rinsed with PBS and membranes were dried at room temperature. Finally, all blots were scanned by a common camera.

2.1.13. Characterization techniques

Absorbance spectra were recorded using UV/Visible double beam spectrophotometer (CECIL 7500 CE, UK) in the wavelength range of 400–800 nm. Water contact angle (WCA) was measured at room temperature using a drop of 3 ml deionized water, put on the glasslide using a microsyringe. The images were captured by “Drop Shape Analysis System”, Kru¨ss G10 system. FTIR-ATR spectra (Alpha-P model, Bruker, Germany) of each sample were acquired in the range of 4000–400 cm^{-1} on a Tensor 27 spectrometer. Size based on z-average and Zeta potential of the GNPs was carried out by photo-correlation spectroscopy (PCS) (Zetasizer Nano ZS, Malvern Instruments, UK). Morphology of the surfaces was observed by scanning electron microscopy (SEM), (SEM; 70 EM3200, KYKY Instruments, China). Transmission electron microscope (TEM) image of GNPs was obtained by a LEO 906, Zeiss-Leica Cooperation, Germany. The average diameters of nanoparticles determined using Digimizer software from TEM and SEM.

3. Result and discussion

3.1.1. Characterization of the colloidal CS-GNPs

Colloidal GNPs were synthesized according to a green synthesis method using chitosan as a reducer and stabilizer agent. The chemicals common methods limited due to their toxic nature during the synthesis and in their application prevent their usage in the biomedical field. Green synthesis methods due to developing simple, clean, non-toxic, cost-effective and eco-friendly can be used in biomedical application as well as sensing application [47]. Colloidal CS-GNPs solution appears an intense red color (Fig. 1A; a) and the UV–Vis spectrum of CS-GNPs was shown a characteristic SPR band at 522 nm confirms the spherical morphology of CS-GNPs (Fig. 1B). CS-GNPs showed an average

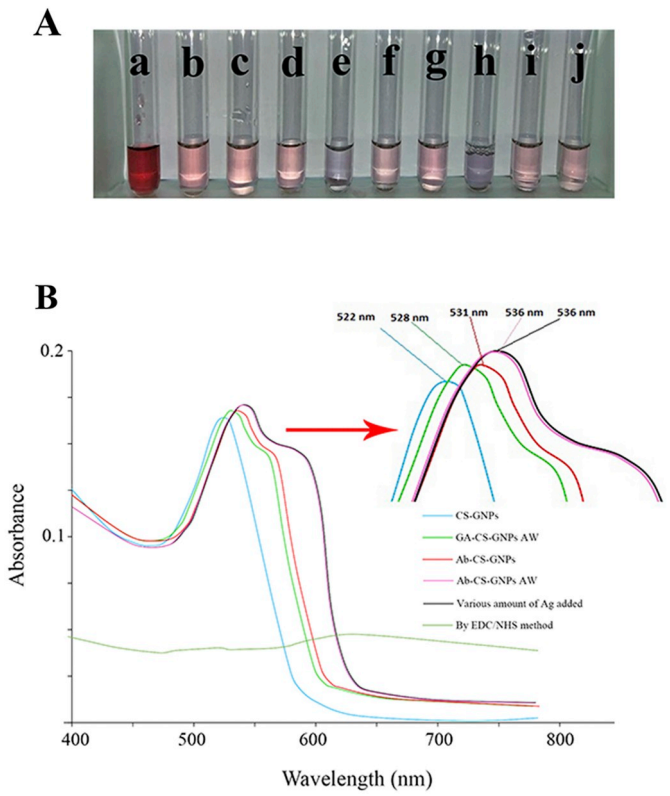

Fig. 1. (A) photograph images colloidal nanoparticles during Ab conjugation process; (a) Synthesized CS-GNPs, (b) Diluted CS-GNPs, (c) GA-CS-GNPs, (d) GA-CS-GNPs after washing, (e) GA-CS-GNPs after addition of Ab 0.003 mg/ml, (f) GA-CS-GNPs after addition of Ab 0.03 mg/ml, (g) GA-CS-GNPs after addition of 0.03 mg/ml, (h) Conjugation by EDC/NHS method, (l) Ab-CS-GNPs after washing (glutaraldehyde method) and (i) after addition of Ag. (B) UV–Vis absorbance spectra of the CS-GNPs during Ab conjugation process and after addition of Ag.

Table 1
Hydrodynamic average diameter, PDI and Zeta Potential of CS-GNPs, GA-CS-GNPs and Ab-CS-GNPs. Values with same superscripts in each column have no significant difference ($p < 0.05$). Data were exhibited as mean ± SD.

Sample	Average diameter (nm)	PDI	Zeta Potential (mv)
CS-GNPs	61 ± 4.08 [a]	0.223 ± 0.07 [a]	+33 ± 7.6 [b]
GA-CS-GNPs	83 ± 6.80 [a, b]	0.241 ± 0.03 [a]	+23 ± 3.6 [b]
Ab-CS-GNPs	109 ± 7.01 [b]	0.282 ± 0.05 [a]	-20 ± 4.02[a]

hydrodynamic diameter of 60 nm with a polydispersity index (PDI) of 0.223 and zeta potential of +33 mV that determined by Zetasizer (Table 1). SEM image confirmed that the CS-GNPs were slightly homogeneous in particle shape and size distribution (Fig. 2A). The SEM particle size distribution histogram (Fig. 2C) showed that the average diameter of CS-GNPs was approximately 40 nm, which is determined by selecting 101 particles randomly by using Digimizer software. Also, the TEM image of colloidal CS-GNPs displayed a lighter contrast chitosan layer around darker GNPs core (zoomed part of Fig. 2B). Results from the present study are consistent with those reported by Kang et al. [48], which showed the presence of thin layer of glycol chitosan around a GNP core. In addition, a similar study was reported by Garatapeh et al., which synthesized CS-GNPs with a thin layer of chitosan was around a GNP core [49]. According to UV/Vis spectra peak that appeared around 522 nm, we expected that the correspondence GNPs diameter should be less than 25 nm [50,51]. These results are in accordance with our results from TEM size distribution histogram of CS-GNPs (Fig. 2D) that shows the average diameter of nanoparticles core with about 17 nm.

However, the reason for the difference in size results of CS-GNPs obtained from SEM and TEM is related to the high thickness of the chitosan layer around GNPs core that is visible in the corresponding zoomed part in Fig. 2B.

Further, the particle size results obtained with the DLS measurement is rather larger than the results achieved by SEM, which may be related to the formation of pseudo-clusters and surface hydration layer on samples [52,53]. Further, the RIS of CS-GNPs was measured that the LSPR shift of the CS-GNPs in the presence of glycerol solutions from 0% to 75% in water shown in Fig. S1; A. The calibration curve received by fitting the LSPR shift vs the refractive index of the various glycerol solutions was shown in Fig. S1; B. This resulted in refractive index sensitivity (RIS) of 60 nm per one refractive index unit. The prepared colloidal CS- GNPs was stable for more than one year that allowed CS-GNPs used for the future conjugation without any stabilizer to store.

3.1.2. Conjugation and characterization of Ab-CS-GNPs

The use of EDC/NHS solution for the conjugation of antibodies on CS-GNPs surface (in all of the samples during and after conjugation process) resulted in aggregation of CS-GNPs (Fig. 1A; h and B). But, the use of GA instead of EDC/NHS method for the conjugation of antibodies on CS-GNPs surface leads to higher stability of CS-GNPs solution compare to EDC/NHS method. This stability can be due to cross-linker nature of GA [54] that can be cross-linked amine groups of chitosan layer on GNPs surface and chitosan like a cage, encloses the GNPs core and lead to stability of CS-GNPs. Due to an aggregation of CS-GNPs by EDC/NHS method we used GA method for the conjugation of Ab to CS-GNPs surface in all of the next steps for biosensing.

Various concentrations of the antibody including 0.003, 0.03 and 0.3 mg/ml was used for conjugation on colloidal CS-GNPs surface to find the optimum amount of Ab (Fig. 1A; c–e). By increasing Ab concentration from 0.003 to 0.3, the stability of CS-GNPs was increased (Fig. 1A; f and g and 5). Aggregation of CS-GNPs after addition of low concentration of Ab (0.003 mg/ml) can be due to the small change in GNPs charge and to follow to flocculation of GNPs [55]. According to the UV/Vis spectra of the CS-GNPs and Ab-CS-GNPs in Fig. 1B, there was 3 nm shifts in the SPR peak after the conjugation of antibodies on CS-GNPs surface. In UV/Vis spectra, the shift from 528 nm to 531 nm, can be caused by the conjugation of the antibodies on colloidal GNPs surface [56]. Also, after addition of GA and centrifuge process appearance a new shoulder peak in UV/Vis spectra that probably occurs because of some aggregation (Fig. 1B). According to the DLS result in Table 1, after functionalized of CS-GNPs by GA (GA-CS-GNPs) an average hydrodynamic diameter and zeta potential was determined 83 nm and + 23 mV, respectively. After Ab conjugation (Ab-CS-GNPs), average-size increase from 83 nm to 109 nm and zeta potential decreased from +23– −20. This changes can be due to immobilization of the antibody on CS-GNPs [57,58]. The RIS of the Ab-CS-GNPs was measured in the presence of glycerol solutions from 0%–75% in water. Fig. S1; C shows the calibration curve of Ab-CS-GNPs that obtained by fitting the LSPR shift vs refractive index of the various glycerol concentrations. A RIS obtained for Ab-CS-GNPs was about 35 nm per refractive index unit (RIU) which was lower than RIS obtained from CS-GNPs (Fig. S1; B). The reason for the decrease in RIS after Ab conjugation was probably due to the increase in thickness of the GNPs coating layer.

HRP protein was used to confirm the attachment of GA on CS-GNPs surface and investigate the capability of CS-GNPs-GA to attach to the amine groups of protein. Fig. S2 showed the HRP-based assays after addition of TMB substrate. The appearance of blue color after HRP conjugation on CS-GNPs (HRP-CS-GNPs) revealed that HRP was conjugated successfully to the surface of the CS-GNPs. BSA conjugated CS-GNP (BSA-CS-GNP) (negative control) showed no color change. Color change in the CS- GNPs sample is due to the enzymatic nature of the colloidal CS-GNPs [39]. Also, in order to confirm the conjugation and function of antibody on CS-GNPs surface, HRP-Tagged-mouse IgG

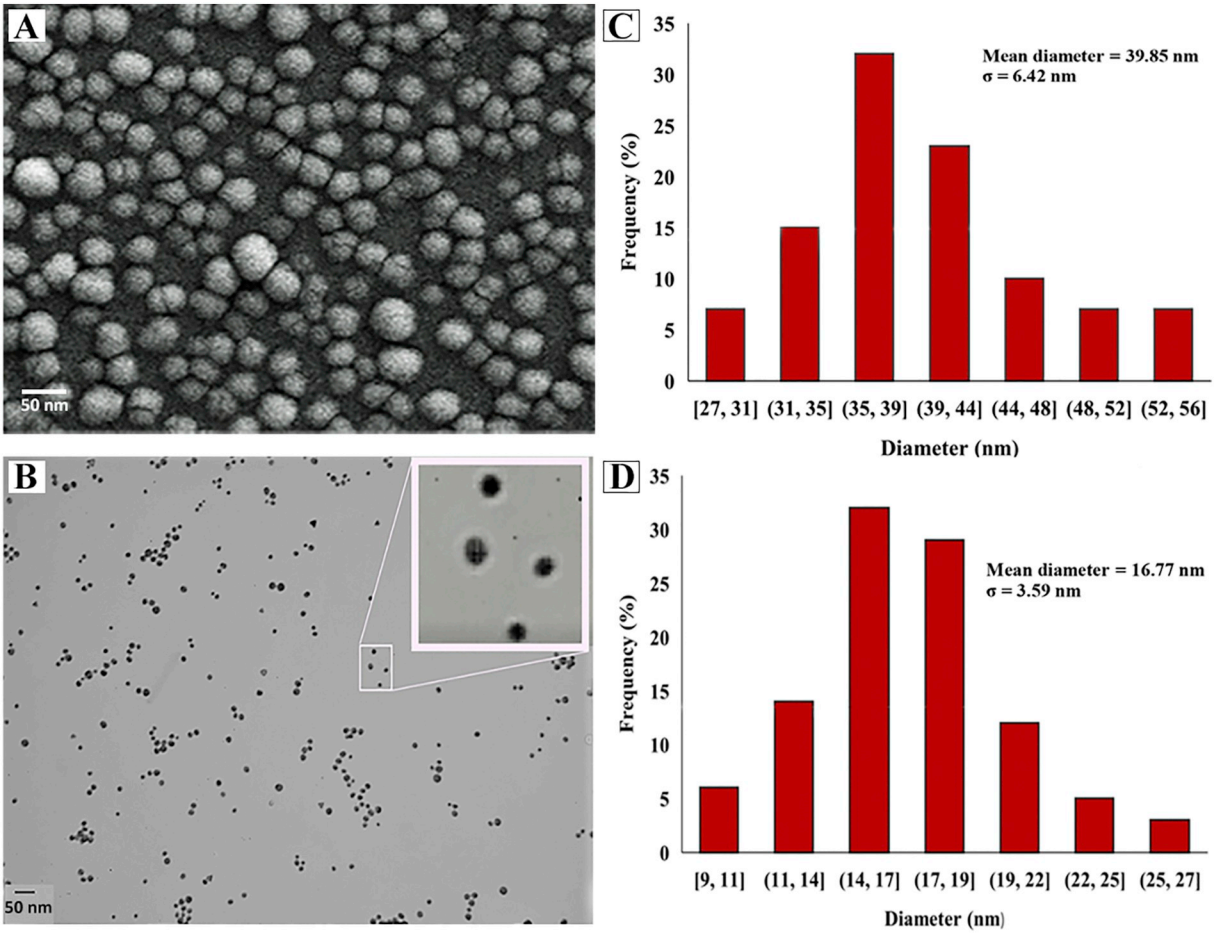

Fig. 2. (A) SEM image, (B) TEM image, (C) SEM size distribution histogram and (D) TEM size distribution histogram of colloidal CS-GNPs.

(HRP-Tagged-Ag) and HRP-Tagged-goat IgG as control were added to the anti-mouse IgG-CS-GNPs (Ab-CS-GNPs) solution. The blue color of the solution in presence of target Ag is due to the presence of HRP that confirmed the antibody-conjugated CS-GNPs is active and can be bind to the target antigen (Fig. S2).

Further, enzyme-labelled antigen (HRP-tagged-mouse IgG) was used to estimate the number of functional antibodies per CS-GNP. In this study, HRP-Tagged-Ag was added to 0.03 and 0.3 mg/ml antibody-functionalized CS-GNP (Ab-CS-GNP), and the bound HRP detected via the enzyme TMB substrate for both samples by use of the standard curve of HRP-tagged-mouse IgG. From this, the relative functional site of antibodies per CS-GNP was estimated. In theory, if we consider the size of nanoparticles 40 nm (by SEM image), the surface area calculated for each nanoparticle is 5024 nm^2. And If the antibody has a size of about 10 nm^2, then the maximum antibodies that can be immobilized on the surface of each nanoparticle calculated around 502.4 [57] (Table 2). In Table 2, the molar concentration of the antibody added to the nanoparticles, the molar concentration of CS-GNPs, the number of antibodies added per nanoparticle, the maximal antibody that can be attached to the surface theoretically, and the molar concentration and number of the antibody functional sites per nanoparticle for two different antibody concentrations that used for functionalization of CS-GNPs have been shown. The number of functional active sites per nanoparticle was estimated at 84.3 and 119 for 0.03 and 0.3 mg/ml Ab functionalized CS-GNP, respectively. The estimated amount of functional Ab per unit area in our results for the 0.3 Ab is greater than the results obtained for the randomly oriented and less than the site-specific oriented method that reported by Van et al. [9]. However, in our developed method due to the high thickness of the chitosan layer around

Table 2
The number of antibody added per colloidal GNP, theoretically maximum capacity of each GNP to functionalized with Ab, and estimated number of functional antibody per GNPs, shown with the molar concentrations of CS-GNP and antibody (0.3 and 0.03 mg/ml).

	Samples	
	Ab 0.3 (mg/ml)-GNP	Ab 0.03 (mg/ml)-GNP
Initial Ab (nM)	2001	200.1
GNP (nM)	0.51	0.51
Initial Number of (Ab)/(GNP)	3923	392.3
Theoretically capacity of (Ab)/(GNP)	502.4	502.4
Functional Ab (nM) by HRP-Ag	61	43
Functional Ab/GNP	119	84.3

GNPs core, the number of functional Ab per CS-GNP core was more than the both mentioned methods previously reported. In addition, conventional methods for conjugating antibodies to the surface of chemically synthesized nanoparticles also have multiple steps that require time and cost [25,30]. However, in our method, without the need for multiple steps, with a simple and rapid method, the antibody is directly conjugated to the GNPs surface. It was concluded that the number of active antibodies per nanoparticle is comparable to costly, toxic and time-consuming methods.

3.1.3. Fabrication of LSPR chip and characterization

The cleaned glasslide was functionalized by APTES and then GNPs directly immobilized on glasslide surface by GA as a linker that coupled

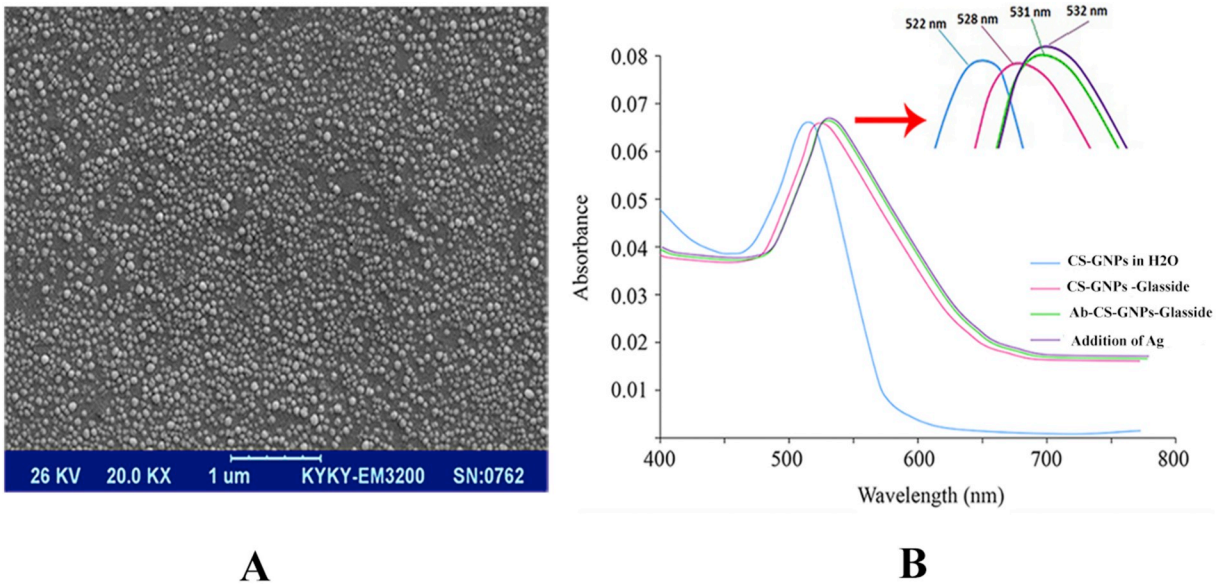

Fig. 3. (A)The SEM image of CS-GNPs immobilized on glasslide surface (CS-GNP-glasslide) and (B) the LSPR spectra of glasslide chip in fabrication process and after addition of Ag.

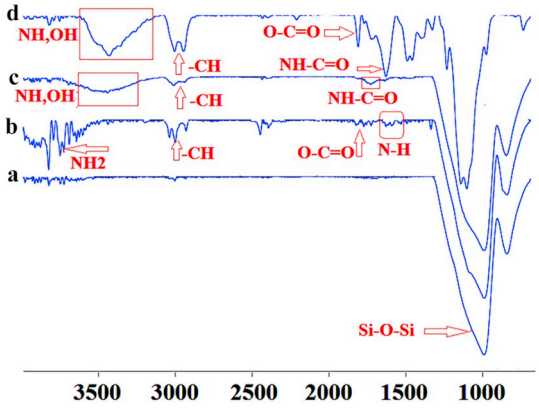

Fig. 4. FTIR spectra of (a) glasslide, (b) APTES-glasslide, (c) CS-glasslide and (d) Ab-CS-glasslide.

amine groups of the APTES-glasslide surface to amine groups of CS-GNPs surface and then again GA functionalized CS-GNPs-glasslide to Ab conjugation. Fig. 3A shows SEM image of CS-GNPs-glasslide that confirm the CS-GNPs successfully immobilized on glasslide surface via a uniform Dispersion whiteout any aggregations. The UV–Vis spectra of CS-GNPs immobilization on glasslide and Ab conjugation process were shown in Fig. 3B. A characteristic LSPR peak at 528 nm confirmed that CS-GNPs immobilized on glasslide surface and a 3 nm shift observed in LSPR peak after Ab conjugation [59]. Fig. 4, was shown FTIR spectra of step by step functionalized glasslide chip. In FTIR spectra of glasslides the very strong peak at the range of 1000–1100 cm^{-1}, was related to the characteristic peak of Si-O-Si. After addition of APTES, the presence of new peaks at 3650, 2830–2950, 1730 and 1590 cm^{-1} was related to stretching vibration of amine, aliphatic –CH, steric carbonyl group and bending vibration of amine groups, respectively. After covalent addition of CS-GNPs to APTES modified glasslides, the presence of a new peak at 1647 cm^{-1} was due to the formation of amide group because of the reaction of glutaraldehyde and amine groups of CS and APTES. Also the wide peak at 3200-3600 cm^{-1} was related to OH and NH groups of chitosan. And at the final step after the addition of Ab the strengthening the peaks at 3200–3600 and 1864–2922 cm^{-1} was due to the presence of amine and acid groups as well as the aliphatic C—H of the antibody. Also, the presences of peaks in 1642, 1690 and 1729 cm-1 were related to amide, esteric and acidic carbonyl group of the Ab and Cs. As a result, the step by step covalently addition of APTES to glasslide, CS-GNP to APTES modified glasslide and finally, addition of Ab to CS-APTES-glasslide was proved by FTIR spectra.

The wetting behaviour of glass substrates surfaces in each step of the fabrication process, were measured by Water contact angle (WCA). For different types of substrate wetting properties are shown in Fig. S3; A. The WCA of 20° was obtained from the cleaned surface treated by piranha solution that shows a hydrophilic surface due to the presence of –OH groups on glasslide surface. After the formation of silane layer (APTES) on the glass substrate, the WCA Increased to 72°, which could be because of exposed silane hydro-carbon groups and amine group instead of –OH groups on glass surface. After activation of the amine group on the glasslide surface by GA, the WCA was reduced to 62° due to exposed aldehyde group of GA. After the presence of CS-GNPs and then Ab on CS-GNPs-glasslide surface, the WCA become 65° and 70°, respectively.

To confirm activation of surface amine groups by glutaraldehyde in each step of the chip fabrication process, and Ab conjugation and capability to Ag binding, HRP and HRP-Tagged-Ag were used respectively. Fig. S3; B, showed the samples after adding one drop of TMB substrate. The observed blue color proves the presence of HRP enzyme. The observation of the blue color in HRP conjugated glasslide (HRP-glasslide) and HRP conjugated CS-GNPs-glasslide (HRP-GNPs-glasslide) samples confirms that GA can successfully activate both of silanized glasslide (APTES-glasslide) and amine group of CS-GNPs-glasslide and attached to amine group of HRP as a protein, respectively (for negative samples, BSA is used instead of HRP). Also, appearance blue color in Ab-GNPs-glasslide sample in the presence of target Ag, confirms the antibodies were conjugated on chip surface and can be bind to target Ag. For negative control HRP-Tagged Goat IgG was added to Ab-GNPs-glasslide instead of target Ag (HRP-Tagged Mouse IgG).

3.1.4. Colorimetric and glasslide-based LSPR sensing capability assessment

As shown in Fig. 1B, after encountered CS-GNPs with PBS and centrifugation, UV–Vis spectra was slightly broadened and red-shift (6 nm) was observed, that can be related to the changes in the stability of CS-GNPs in presence of PBS and centrifugation process. Immediately after antibody (anti IgG) conjugation on CS-GNPs surface (Ab-CS-GNPs) the maximum absorption wavelength (l max) was red-shifted around 3 nm. This red-shift was considered as the evidence of protein

immobilization onto the nanoparticle surface [56]. After removal extra amount of Ab by several times washing (AW), in maximum absorption wavelength of Ab-CS-GNPs, a 5 nm red shift was observed. After addition of antigen (IgG) (at all concentrations) to the Ab-CS-GNPs solution, the absorption wavelength of Ab-CS-GNPs was not changed. This limitation can be due to the attachment of a small number of antigens to antibodies in the CS-GNPs surface or a decrease in the LSPR sensitivity to change the refractive index. Fig. S1; shows that after the conjugation of Ab on CS-GNPs surface, the refractive index sensitivity decreases.

The LSPR peak of CS-GNPs after immobilization on glasslide showed a red-shift of about 6 nm and after the presence of PBS and washing process, LSPR peak compare to the colloidal CS-GNPs not shifted (Fig. 3B). Also after antibody conjugation on CS-GNPs immobilized glasslide (Ab-CS-GNPs-glass), similar to colloidal Ab-CS-GNPs, the LSPR peak shifted 3 nm and after addition of antigen at various concentrations the LSPR peak not changed significantly (about 1 nm).

The shift in LSPR peak upon binding one layer adsorbate has been expressed by *Equation*$_1$ [60,61];

$$\lambda_{max} = m\Delta\eta\,[1 - exp\,(-2d/l_d)] \quad (1)$$

where m is the sensitivity of RI, ($\Delta\eta$) is the difference RI between the layer coating the nanoparticles (ηA) and the solvent environment (ηE), d is the optical thickness of the coating layer, and l_d is the Plasmon effective decay length. Also, if the second layer contains the analyte, (e.g., a specific antigen), that will bind to the adsorbate layer, and a change in the LSPR will be detected. The LSPR shift in such a scenario is expressed by *Equation*$_2$ [62,63];

$$\lambda_{max} = m\Delta\eta\ exp\,(-2d_1/l_d)\,[1 - exp\,(-2d_2/l_d)] \quad (2)$$

where *d1* is the thicknesses of the first adsorbate layer and *d2* is the thicknesses of the second layer (analyte). According to Eq. (2), a maximal response to the antigen binding one has to maximize the refractive index sensitivity (m) and match the Plasmon effective decay length (l_d) to the analyte (d_2) and adsorbate layer interface dimensions (Scheme 1A). Therefore, if the decay length l_d is much large with respect to the optical layer thickness, the analyte will occupy a little part of the sensing volume, that lead to a weak response (Scheme 1C). On the other hand, if the decay length l_d is small compared to the optical layer thickness, the rapid decay, leading to a weakly response to the analyte binding (Scheme 1B). According to the TEM image in Fig. 2B, which a thicker layer of chitosan surrounds the GNPs, the weak response to the antigen binding in our work is due to the long distance of the detection interface from the surface of the GNPs core which is in accordance with the results of previous works reported on the effect of adsorbed layer thickness in LSPR based sensing [61,62,64,65].

3.1.5. Dot-blot based detection assessment

The fabricated Ab-CS-GNPs were used as an immunoprobe for detection of the target antigen spotted on NC paper. In graphical abstract A, illustrates the designed immunoprobe and sensing format for target antigen detection. Two concentrations of anti-mouse IgG (Ab) (0.3 and 0.03 mg/ml) which after conjugation lead to a stable immunoprobe (Fig. 1A) were used to detect different concentrations of (100, 10, 1, and 0.1 μg/ml) spotted mouse IgG (Ag) on NC paper (Fig. 5) in order to ascertain the sensitivity of detection by the naked eye. Although the number of functional active sites in 0.3 mg/ml Ab conjugated CS-GNPs is greater than 0.03 mg/ml Ab conjugated CS-GNPs (Table 2), the LOD for both concentrations (0.3and 0.03 mg/ml) without any signal enhancement obtained 1 μg/ml (~6 nM). This is probably due to the presence of enough antibody on the CS-GNP surface in both concentrations for detection of target Ag (Table 2). Also, we used goat IgG as a negative control and the result showed after placing the NC paper in the Ab-CS-GNPs solution, spots not a colored (Fig. 5). That proves the Ab-CS-GNPs have the specificity required for detection. Due to variations in the color intensity of the dots at different concentrations, this method can be quantified using a computer program for color intensity analysis [66]. It can also be used in clinical diagnostic programs by change of conjugated antibody that bind to a specific antigen. In this work without using any signal enhancement, LOD was 1 μg/ml (~6 nM), that was stronger than a similar study used a designed Fischer carbene complex for conjugation anti-rabbit IgG to the detection of rabbit IgG on NC membrane [67]. Anyway, our purpose was to develop

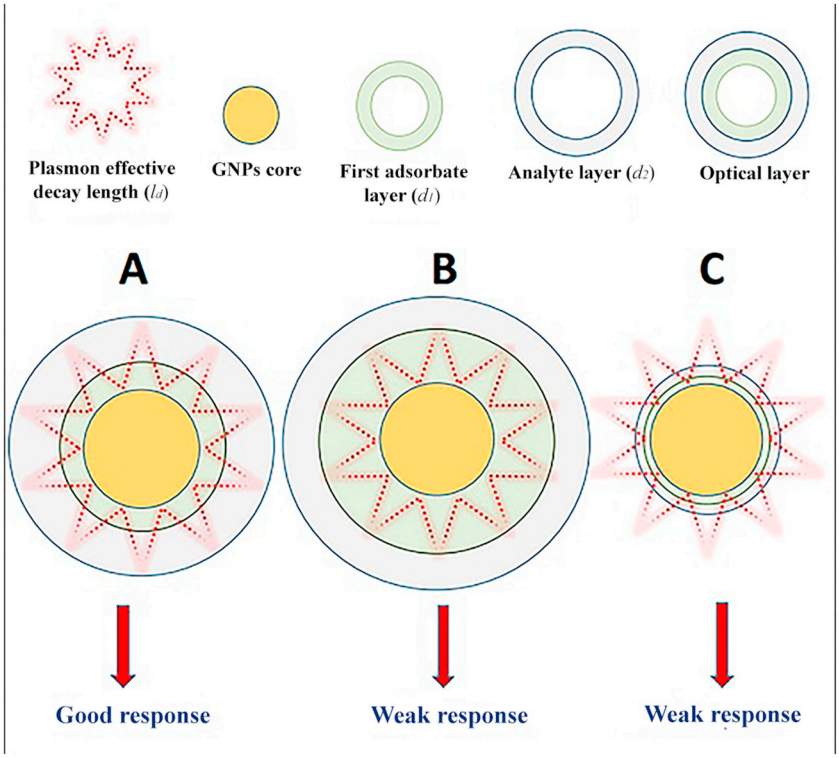

Scheme 1. Schematic illustration of the dependence between Plasmon effective decay length (ld) and absorbed layer diameter to create a response

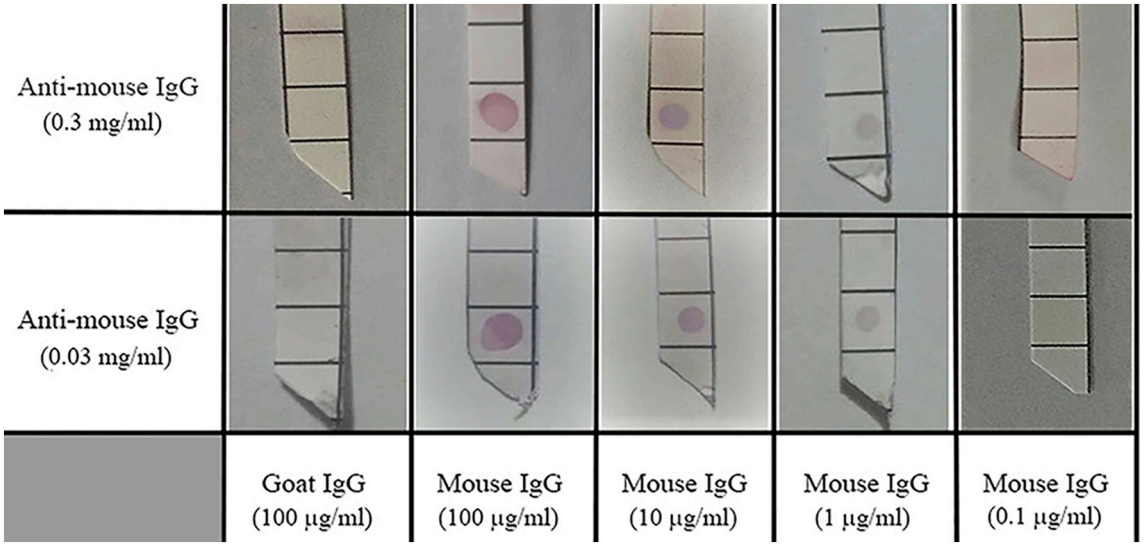

Fig. 5. Photograph image of Dot-blot assay by two concentration of conjugated antibody on CS-GNPs surface to detection of Ag at various dilutions.

a low cost, simple, and safe technique to antibody conjugation on GNPs surface which was appropriate to visual detection and we were successful in doing so.

4. Conclusion

In this work, we have developed a novel approach to directly immobilize the antibody on the surface of chitosan-based green synthesized GNPs through covalent bonding. The advantages of this method in comparison with other common methods include the use of a green method for the synthesis of GNPs, its low cost, simplicity (no need for ligand exchange) and prolonged functionality. The capability of CS-GNPs in antigen detection was evaluated through three types of optical immunoassay-based antigen-antibody interaction (colorimetric, glass-slide-based LSPR and paper-based dot-blot). In colorimetric and glass-slide-based LSPR detection systems, the response from the antibody-antigen binding was not significant, this can be attributed to the thickness of the chitosan layer on the GNPs surface [62]. But, in a paper-based detection method, LOD was 1 µg/ml, This LOD is lower than the LOD in a similar work that applied Fischer carbene complex for Ab conjugation [67]. This result indicates that when using GNPs in optical label-free detection systems (such as colorimetric and LSPR in our work), special attention should be paid to the thickness of the coating layer on GNPs surface and the distance of interaction line (Ab-Ag) from the GNPs core. Also the high potential of Ab-CS-GNPs as a green immunoprobe for paper-based immunoassays indicates Ab-CS-GNPs can be used in sandwich-like immunoassay systems that apply GNPs as a label for Ab. In the sandwich format, conjugated label-antibody binds to specific antigens to form an antibody-antigen complex. Then, this complex binds to a specific antibody and forms a sandwich like antigen-antibody system. The result can be perceived directly where the presence of a visual color in the tests [68]. Furthermore, the sensitivity of this detection system can be possibly improved by the use of protein A/G to site-specific oriented Ab immobilization on CS-GNPs and application of signal enhancement methods [9,69].

Acknowledgement

This study was financially supported by a grant [NO: 95/2-3/4] from Faculty of Advanced Medical Science, Tabriz University of Medical Sciences, Tabriz, Iran.

Declaration of Competing Interest

None.

Appendix A. Supplementary data

Supplementary data to this article can be found online at https://doi.org/10.1016/j.colcom.2019.100207.

References

[1] J. Gao, et al., Colloidal stability of gold nanoparticles modified with thiol compounds: bioconjugation and application in cancer cell imaging, Langmuir 28 (9) (2012) 4464–4471.
[2] R. Marega, et al., Antibody-functionalized polymer-coated gold nanoparticles targeting cancer cells: an in vitro and in vivo study, J. Mater. Chem. 22 (39) (2012) 21305–21312.
[3] M. Lisa, et al., Gold nanoparticles based dipstick immunoassay for the rapid detection of dichlorodiphenyltrichloroethane: an organochlorine pesticide, Biosens. Bioelectron. 25 (1) (2009) 224–227.
[4] K. Sokolov, et al., Real-time vital optical imaging of precancer using anti-epidermal growth factor receptor antibodies conjugated to gold nanoparticles, Cancer Res. 63 (9) (2003) 1999–2004.
[5] T. Dreifuss, et al., Correction: a challenge for theranostics: is the optimal particle for therapy also optimal for diagnostics? Nanoscale 8 (33) (2016) (15357–15357).
[6] M.S. Muthu, P. Agrawal, S. Singh, Theranostic nanomedicine of gold nanoclusters: an emerging platform for cancer diagnosis and therapy, Nanomedicine (Lond) 11 (4) (2016) 327–330.
[7] K. Saha, et al., Gold nanoparticles in chemical and biological sensing, Chem. Rev. 112 (5) (2012) 2739–2779.
[8] S. Su, et al., Shape-controlled gold nanoparticles supported on MoS 2 nanosheets: synergistic effect of thionine and MoS 2 and their application for electrochemical label-free immunosensing, Nanoscale 7 (45) (2015) 19129–19135.
[9] S. Van Der Heide, D.A. Russell, Optimisation of immuno-gold nanoparticle complexes for antigen detection, J. Colloid Interface Sci. 471 (2016) 127–135.
[10] C.J. Ackerson, et al., Rigid, specific, and discrete gold nanoparticle/antibody conjugates, J. Am. Chem. Soc. 128 (8) (2006) 2635–2640.
[11] P. Ciaurriz, et al., Comparison of four functionalization methods of gold nanoparticles for enhancing the enzyme-linked immunosorbent assay (ELISA), Beilstein J. Nanotechnol. 8 (2017) 244.
[12] S. Neethirajan, et al., Nano-biosensor platforms for detecting food allergens–new trends, Sens. Bio-Sens. Res. 18 (2018) 13–30.
[13] P. Damborský, J. Švitel, J. Katrlík, Optical biosensors, Essays Biochem. 60 (1) (2016) 91–100.
[14] X. Fan, et al., Sensitive optical biosensors for unlabeled targets: a review, Anal. Chim. Acta 620 (1–2) (2008) 8–26.
[15] S.K. Pandey, et al., A gold nanoparticles based immuno-bioprobe for detection of Vi capsular polysaccharide of *Salmonella enterica* serovar Typhi, Mol. Biosyst. 8 (7) (2012) 1853–1860.
[16] C. Thiruppathiraja, et al., An enhanced immuno-dot blot assay for the detection of white spot syndrome virus in shrimp using antibody conjugated gold nanoparticles probe, Aquaculture 318 (3–4) (2011) 262–267.
[17] F. Xia, et al., Colorimetric detection of DNA, small molecules, proteins, and ions

using unmodified gold nanoparticles and conjugated polyelectrolytes, Proc. Natl. Acad. Sci. 107 (24) (2010) 10837–10841.
[18] H. Aldewachi, et al., Gold nanoparticle-based colorimetric biosensors, Nanoscale 10 (1) (2018) 18–33.
[19] V. Nanduri, et al., SPR biosensor for the detection of *L. monocytogenes* using phage-displayed antibody, Biosens. Bioelectron. 23 (2) (2007) 248–252.
[20] J. Jatschka, et al., Propagating and localized surface plasmon resonance sensing—a critical comparison based on measurements and theory, Sensing Bio-Sensing Res. 7 (2016) 62–70.
[21] X. Mao, et al., Molecular beacon-functionalized gold nanoparticles as probes in dry-reagent strip biosensor for DNA analysis, Chem. Commun. (21) (2009) 3065–3067.
[22] R. Gillibert, M.N. Triba, M.L. de la Chapelle, Surface enhanced Raman scattering sensor for highly sensitive and selective detection of Ochratoxin A, Analyst 143 (1) (2018) 339–345.
[23] M. Zhang, et al., A biosensor for cholesterol based on gold nanoparticles-catalyzed luminol electrogenerated chemiluminescence, Biosens. Bioelectron. 32 (1) (2012) 288–292.
[24] Z. Liu, et al., A label-free fluorescence biosensor for highly sensitive detection of lectin based on carboxymethyl chitosan-quantum dots and gold nanoparticles, Anal. Chim. Acta 932 (2016) 88–97.
[25] J. Baniukevic, et al., Application of oriented and random antibody immobilization methods in immunosensor design, Sens. Actuators B 189 (2013) 217–223.
[26] K. Yoshimoto, et al., Direct observation of adsorption-induced inactivation of antibody fragments surrounded by mixed-PEG layer on a gold surface, J. Am. Chem. Soc. 132 (23) (2010) 7982–7989.
[27] J. Goossens, et al., Functionalization of gold nanoparticles with nanobodies through physical adsorption, Anal. Methods 9 (23) (2017) 3430–3440.
[28] H. Zhang, et al., Studies of gold nanorod-iron oxide nanohybrids for immunoassay based on SPR biosensor, Talanta 125 (2014) 29–35.
[29] S. Wang, et al., Rapid colorimetric identification and targeted Photothermal lysis of Salmonella Bacteria by using bioconjugated oval-shaped gold nanoparticles, Chem. A Eur. J. 16 (19) (2010) 5600–5606.
[30] M.H. Jazayeri, et al., Various methods of gold nanoparticles (GNPs) conjugation to antibodies, Sensing Bio-Sensing Res. 9 (2016) 17–22.
[31] R.A. Zangmeister, et al., Electrochemical study of chitosan films deposited from solution at reducing potentials, Electrochim. Acta 51 (25) (2006) 5324–5333.
[32] R. Karthikeyan, et al., Functionalization of electrochemically deposited chitosan films with alginate and Prussian blue for enhanced performance of microbial fuel cells, Electrochim. Acta 112 (2013) 465–472.
[33] L. Sun, et al., One pot synthesis of gold nanoparticles using chitosan with varying degree of deacetylation and molecular weight, Carbohydr. Polym. 178 (2017) 105–114.
[34] H. Huang, X. Yang, Synthesis of chitosan-stabilized gold nanoparticles in the absence/presence of tripolyphosphate, Biomacromolecules 5 (6) (2004) 2340–2346.
[35] Z. Chen, et al., Chitosan-capped gold nanoparticles for selective and colorimetric sensing of heparin, J. Nanopart. Res. 15 (9) (2013) 1930.
[36] D.R. Bhumkar, et al., Chitosan reduced gold nanoparticles as novel carriers for transmucosal delivery of insulin, Pharm. Res. 24 (8) (2007) 1415–1426.
[37] X. Zhou, et al., The effect of conjugation to gold nanoparticles on the ability of low molecular weight chitosan to transfer DNA vaccine, Biomaterials 29 (1) (2008) 111–117.
[38] S.N. Tammam, et al., Chitosan gold nanoparticles for detection of amplified nucleic acids isolated from sputum, Carbohydr. Polym. 164 (2017) 57–63.
[39] C. Jiang, et al., Chitosan–gold nanoparticles as peroxidase mimic and their application in glucose detection in serum, RSC Adv. 7 (70) (2017) 44463–44469.
[40] L. He, et al., Chitosan stabilized gold nanoparticle based electrochemical ractopamine immunoassay, Microchim. Acta 184 (8) (2017) 2919–2924.
[41] H. Ma, et al., Label-free immunosensor based on one-step electrodeposition of chitosan-gold nanoparticles biocompatible film on Au microelectrode for determination of aflatoxin B1 in maize, Biosens. Bioelectron. 80 (2016) 222–229.
[42] C. Xiang, et al., Sensitive electrochemical detection of Salmonella with chitosan–gold nanoparticles composite film, Talanta 140 (2015) 122–127.
[43] X. Liu, et al., Extinction coefficient of gold nanoparticles with different sizes and different capping ligands, Colloids Surf. B Biointerfaces 58 (1) (2007) 3–7.
[44] T. Hendel, et al., In situ determination of colloidal gold concentrations with UV–Vis spectroscopy: limitations and perspectives, Anal. Chem. 86 (22) (2014) 11115–11124.
[45] S. Narayan, et al., BSA binding to silica capped gold nanostructures: effect of surface cap and conjugation design on nanostructure–BSA interface, RSC Adv. 4 (3) (2014) 1412–1420.
[46] H. Chen, et al., Stabilization of gold nanoparticles on glass surface with poly-dopamine thin film for reliable LSPR sensing, J. Colloid Interface Sci. 460 (2015) 258–263.
[47] A.I. Usmanac, A.A. Aziza, O.A. Noqtab, Application of Green Synthesis of Gold Nanoparticles: A Review, (2017).
[48] B. Kang, et al., Carbohydrate nanocarriers in biomedical applications: functionalization and construction, Chem. Soc. Rev. 44 (22) (2015) 8301–8325.
[49] A. Gharatape, et al., A novel strategy for low level laser-induced plasmonic photothermal therapy: the efficient bactericidal effect of biocompatible AuNPs@(PNIPAAM-co-PDMAEMA, PLGA and chitosan), RSC Adv. 6 (112) (2016) 110499–110510.
[50] S.N. Tammam, et al., Chitosan gold nanoparticles for detection of amplified nucleic acids isolated from sputum, Carbohydr. Polym. 164 (2017) 57–63.
[51] P.N. Njoki, et al., Size correlation of optical and spectroscopic properties for gold nanoparticles, J. Phys. Chem. C 111 (40) (2007) 14664–14669.
[52] R. Salehi, S. Rasouli, H. Hamishehkar, Smart thermo/pH responsive magnetic nanogels for the simultaneous delivery of doxorubicin and methotrexate, Int. J. Pharm. 487 (1–2) (2015) 274–284.
[53] J. Lin, et al., Functionally modified monodisperse core–shell silica nanoparticles: silane coupling agent as capping and size tuning agent, Colloids Surf. A Physicochem. Eng. Asp. 411 (2012) 111–121.
[54] O.A. Monteiro Jr., C. Airoldi, Some studies of crosslinking chitosan–glutaraldehyde interaction in a homogeneous system, Int. J. Biol. Macromol. 26 (2–3) (1999) 119–128.
[55] I. Safenkova, A. Zherdev, B. Dzantiev, Factors influencing the detection limit of the lateral-flow sandwich immunoassay: a case study with potato virus X, Anal. Bioanal. Chem. 403 (6) (2012) 1595–1605.
[56] W.P. Hall, S.N. Ngatia, R.P. Van Duyne, LSPR biosensor signal enhancement using nanoparticle− antibody conjugates, J. Phys. Chem. C 115 (5) (2011) 1410–1414.
[57] N. Mustafaoglu, T. Kiziltepe, B. Bilgicer, Site-specific conjugation of an antibody on a gold nanoparticle surface for one-step diagnosis of prostate specific antigen with dynamic light scattering, Nanoscale 9 (25) (2017) 8684–8694.
[58] M.O. Ijeh, Covalent Gold Nanoparticle-Antibody Conjugates for Sensivity Improvement in LFIA, (2011).
[59] M. Yüce, H. Kurt, How to make nanobiosensors: surface modification and characterisation of nanomaterials for biosensing applications, RSC Adv. 7 (78) (2017) 49386–49403.
[60] A. Vaskevich, I. Rubinstein, Localized surface plasmon resonance (LSPR) spectroscopy in biosensing, Handbook of Biosensors and Biochips, 2007.
[61] M.D. Malinsky, et al., Chain length dependence and sensing capabilities of the localized surface plasmon resonance of silver nanoparticles chemically modified with alkanethiol self-assembled monolayers, J. Am. Chem. Soc. 123 (7) (2001) 1471–1482.
[62] O. Kedem, et al., Sensitivity and optimization of localized surface plasmon resonance transducers, ACS Nano 5 (2) (2011) 748–760.
[63] J.C. Riboh, et al., A nanoscale optical biosensor: real-time immunoassay in physiological buffer enabled by improved nanoparticle adhesion, J. Phys. Chem. B 107 (8) (2003) 1772–1780.
[64] L. Song, et al., Amplifying the signal of localized surface plasmon resonance sensing for the sensitive detection of *Escherichia coli* O157: H7, Sci. Rep. 7 (1) (2017) 3288.
[65] J. Jatschka, et al., Propagating and localized surface plasmon resonance sensing — a critical comparison based on measurements and theory, Sensing Bio-Sensing Res. 7 (2016) 62–70.
[66] Y.-Y. Chen, et al., Functional gold nanoparticles coupled with microporous membranes: a flow controlled assay for colorimetric visualization of proteins, Analyst 139 (22) (2014) 5977–5982.
[67] N. Ray, S. Sawoo, A. Sarkar, Fischer carbene complex with hydrophilic OEG-tentacles decorates antibody surface with in situ generated gold nanoparticles for rapid, sensitive, visual detection of proteins, Anal. Methods 6 (2) (2014) 351–354.
[68] M. Yahaya, et al., 6 Multiplexing of Nanoparticles-Based Lateral Flow Immunochromatographic Strip: A Review, (2018).
[69] X. Cao, Y. Ye, S. Liu, Gold nanoparticle-based signal amplification for biosensing, Anal. Biochem. 417 (1) (2011) 1–16.